GeoHealth

RESEARCH ARTICLE

10.1029/2025GH001604

Key Points:

- Wet bulb globe temperature exceeds safe limits in key harvest months, putting farmworkers at high risk of heat-related illness
- Heat risk varies by crop, season, workload, and shift timing; current work schedules often include the hottest hours of the day
- Proposed heat stress mitigation strategies include adjusting work hours and adopting variable rest-breaks, especially in high-risk crop zones

Supporting Information:

Supporting Information may be found in the online version of this article.

Correspondence to:

S. P. Parajuli,
psagar@utexas.edu

Citation:

Parajuli, S. P., Biggs, T., Monteverde, C., Ciborowski, H., Lopez Galvez, N., Quintana, P. J. E., et al. (2026). High-resolution modeling of wet bulb globe temperature reveals substantial heat risks across crops and work shifts among agricultural workers in southern California. *GeoHealth*, *10*, e2025GH001604. https://doi.org/10.1029/2025GH001604

Received 17 JUL 2025
Accepted 30 APR 2026

Author Contributions:

Conceptualization: Sagar P. Parajuli, Trent Biggs, Nicolas Lopez Galvez, Penelope J. E. Quintana
Data curation: Corrie Monteverde
Formal analysis: Sagar P. Parajuli, Corrie Monteverde
Funding acquisition: Trent Biggs, Nicolas Lopez Galvez, Penelope J. E. Quintana, Fernando De Sales, Miguel Angel Zavala Perez, Charles Jones

High-Resolution Modeling of Wet Bulb Globe Temperature Reveals Substantial Heat Risks Across Crops and Work Shifts Among Agricultural Workers in Southern California

Sagar P. Parajuli[1], Trent Biggs[1], Corrie Monteverde[1], Haley Ciborowski[2], Nicolas Lopez Galvez[2], Penelope J. E. Quintana[2], Fernando De Sales[1], Miguel Angel Zavala Perez[3], Callum Thompson[4], and Charles Jones[4]

[1]Department of Geography, San Diego State University, San Diego, CA, USA, [2]School of Public Health, San Diego State University, San Diego, CA, USA, [3]San Diego State University Imperial Valley Campus, Calexico, CA, USA, [4]University of California, Santa Barbara, Santa Barbara, CA, USA

Abstract Farmworkers are particularly vulnerable to heat stress, which can escalate into heat-related illnesses such as heat exhaustion or heat stroke, and can also impact productivity loss. Heat exposure varies considerably depending on season, work-shift timing, acclimatization, and workload. We examine the frequency of heat stress exceedance in the Imperial and Coachella Valleys of southern California using wet bulb globe temperature (WBGT) calculated using the outputs from Weather Research and Forecasting (WRF) model for a reference year of 2020. The critical WBGT threshold of 80℉ is exceeded for more than 500 hr in August, with considerable exceedance in all key harvesting months of April, May, and June. The threshold is exceeded most frequently in August, with daytime (nighttime) exceedance of 96.3% (38.0%) in the Imperial and 72.5% (11.9%) in the Coachella Valleys. Occupational WBGT limits are also exceeded in most crop environments for unacclimatized workers, and even for acclimatized workers during date and sugarcane harvests. Adjusting the work schedule to an early morning or late evening shift can reduce workers' productivity loss by up to 40%. Based on our findings, we propose several strategies to mitigate heat risks among farmworkers: (a) adjusting work hours to include cooler morning or evening hours (b) using WBGT instead of air temperature to monitor heat exposure (c) adopting variable rest-break schedules (d) reducing nighttime heat exposure during summer to allow recovery from daytime heat (e) taking extra precaution in high-risk crop zones (f) avoiding nighttime irrigation during summer, and (g) revising thresholds and definitions used to identify heatwaves.

Plain Language Summary Farmworkers are at high risk of heat stress because they work outdoors for prolonged hours under strenuous conditions. This can lead to serious illnesses such as heat stroke and can reduce productivity. We examined how often heat exposure exceeds safety limits in California's agricultural heartlands, the Imperial and Coachella Valleys, using the Wet-Bulb Globe Temperature (WBGT), a scientific heat metric. We found that WBGT exceeded the safety limit for hundreds of hours during key harvest months such as April, May, and June. Based on our results, we recommend several heat-exposure mitigation strategies to protect farmworkers: (a) adjusting work hours to include cooler morning or evening periods; (b) using WBGT rather than air temperature to monitor heat exposure; (c) adopting a variable rest-break schedule; (d) reducing nighttime heat exposure during summer to support recovery from daytime heat; (e) taking extra precautions in high-risk crop zones; (f) avoiding nighttime irrigation during summer; and (g) revising definitions used to identify heatwaves.

1. Introduction

Heat stress is a critical threat to the health of outdoor workers, including farmworkers (Fatima et al., 2021; Jackson & Rosenberg, 2010). Heat stress has serious health consequences, from heat-related illnesses to death due to heat strokes (Moyce et al., 2017; Ostro et al., 2009; Smith et al., 2022). Heat stress also affects worker productivity (Parsons et al., 2022) as workers slow down to cope with heat and to reduce the risk of injury (Roson & Sartori, 2016; Tawatsupa et al., 2013). Meteorology-based metrics, including air temperature (CCR, 2005), heat index (Rothfusz, 1990), and wet bulb globe temperature (WBGT) (Kong & Huber, 2022; Parajuli et al., 2024) can provide proxies of heat stress exposure for workers, but farmworkers have highly variable work shifts (Mitchell et al., 2018), including night-time work (Tan & Bogage, 2023), that vary by crop and need to be accounted for when tabulating heat exposure metrics.

Investigation: Sagar P. Parajuli, Haley Ciborowski, Nicolas Lopez Galvez, Penelope J. E. Quintana
Methodology: Sagar P. Parajuli, Corrie Monteverde, Haley Ciborowski, Nicolas Lopez Galvez, Fernando De Sales, Miguel Angel Zavala Perez, Callum Thompson, Charles Jones
Project administration: Trent Biggs
Software: Sagar P. Parajuli
Supervision: Trent Biggs
Validation: Sagar P. Parajuli
Visualization: Sagar P. Parajuli, Corrie Monteverde
Writing – original draft: Sagar P. Parajuli
Writing – review & editing: Trent Biggs, Haley Ciborowski, Nicolas Lopez Galvez, Penelope J. E. Quintana, Fernando De Sales, Miguel Angel Zavala Perez, Callum Thompson, Charles Jones

Heat exposure also impacts labor productivity. Although employers might perceive that taking longer rest breaks could reduce productivity, there is limited evidence and lack of studies on the impact of rest breaks on productivity (Faucett et al., 2007). Several previous studies have quantified the loss of productivity at higher heat stress levels under future climate scenarios (Dunne et al., 2013; Matsumoto et al., 2021; Saeed et al., 2022). Multiple labor response functions (LRFs) have been developed to estimate the impact of heat stress on labor productivity in terms of WBGT (Bröde et al., 2018; d'Ambrosio Alfano et al., 2014; Kjellstrom et al., 2018; Malchaire, 1979; Sahu et al., 2013; Wyndham, 1969). Different crops have different greenness, plant density, plant heights, and planting/harvesting seasons, which can impact the land surface temperature, air temperature, and humidity levels (Bonan, 2008; Parajuli & Yang, 2017). Therefore, heat exposure is expected to vary across different crop environments. Labor requirements also vary significantly across different crops due to differences in cultivation practices and harvesting methods (Mohammadian et al., 2020; Pan et al., 2021). High-value or perishable crops such as fruits, vegetables, and specialty crops often require intensive manual labor for tasks like transplanting, hand weeding, selective harvesting, and packaging. Work shifts vary widely by crop: greens may be harvested at night to maintain crop turgor and flavor, while other crops, such as orchard crops, may be harvested during the day due to lighting and safety challenges at night (Mayer, 2023). Detailed information on farming work schedules are often not readily available, complicating the calculation of heat indices during work hours.

The Imperial and Coachella Valleys (ICV) have some of the largest agricultural fields in California, supplying a large fraction of the fruits and vegetables consumed in the US (CDFA, 2023). Imperial County also has the highest heat-related illness rate reported in California (Heinzerling et al., 2020). About 20,000 farmworkers are active in the ICV region in any given month (CES, 2020), which is about 30% of California's total farm employment (Martin et al., 2017). Most of the farmworkers working in the region are seasonal migrant workers of Hispanic origin coming from the bordering town of Mexicali, Mexico (Vega-Arroyo et al., 2019). Despite the presence of a large number of outdoor farmworkers, a comprehensive spatio-temporal evaluation of heat exposure in the ICV region is lacking, particularly during the period of intensive harvesting, as opposed to the more common summer periods (Thompson et al., 2025).

Various crops are grown in the ICV, each with different planting and harvesting seasons. April has the highest greenness in the year in the ICV fields as per the leaf area index (LAI) data in the study area (Parajuli et al., 2024). Major winter crops include lettuce, cauliflower, kale, and broccoli; spring crops include onions, citrus, and carrots; summer crops include melons, corn, and wheat and summer-to-fall crops include dates, lemons, and olives, while other crops like sugarcane, alfalfa, and animal fodder are grown all year round (Parajuli et al., 2025).

The Wet Bulb Globe Temperature (WBGT) is a widely accepted international standard for measuring heat stress (ISO, 2017), which uses all key meteorological factors affecting heat stress, including air temperature, humidity, solar and thermal radiation, and wind speed. The WBGT can be directly measured using WBGT monitors (Clark & Konrad, 2024) or estimated using meteorological data and weather model outputs with reasonable accuracy (Kong & Huber, 2022, 2024; Liljegren et al., 2008; Parajuli et al., 2024). The WBGT for outdoor environment is given by the following equation (Budd, 2008; Yaglou & Minard, 1957):

$$\mathrm{WBGT} = 0.7 \times \mathrm{WBT} + 0.2 \times \mathrm{BGT} + 0.1 \times \mathrm{DBT} \tag{1}$$

where WBT is the natural wet-bulb temperature, BGT is the black globe temperature and DBT is the dry-bulb temperature (or simply air temperature measured in weather stations).

In this work, we examine how often thresholds of heat stress are exceeded in farmworkers' work environment in the ICV region (Figure 1) using WBGT as a heat stress indicator. We calculate WBGT using outputs from a validated Weather Research and Forecasting (WRF) model, which is a widely used numerical model both for research (Parajuli et al., 2022) and operational weather forecasting (Cobb et al., 2023). We use the gold-standard method for calculating WBGT (Liljegren et al., 2008), recently implemented in Python (PyWBGT) (Kong & Huber, 2022). We specifically use PyWBGT's WBGT_GCM formulation, which modifies the Liljegren et al. method to include longwave radiation in addition to shortwave radiation. Note that another computationally more efficient approximation is also available from the same authors (Kong & Huber, 2024), which we do not use. Our model includes the effects of irrigation, which is a key modulator of heat stress in the region (Parajuli et al., 2024).

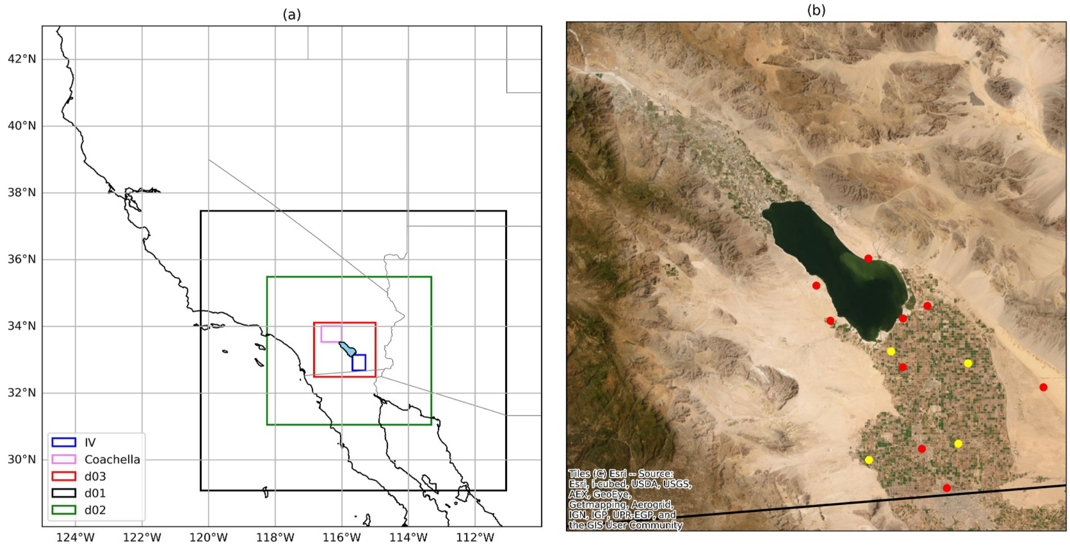

Figure 1. (a) WRF model domain configuration showing the region of interest (d03) over the Imperial and Coachella Valleys and (b) the location of stations from CIMIS (yellow) and CARB (red) networks used for model validation plotted on a satellite image of the region with the Salton Sea at the center.

The use of WRF outputs enables calculation of heat stress exceedances across the entire ICV region at high spatial and temporal resolution. We explore the following specific research questions:

1. How often are the heat stress limits exceeded during the harvesting seasons in Imperial and Coachella Valleys?
2. How does heat exposure vary by work hours, seasons, and crop types?
3. What are possible heat stress mitigation strategies for farmworkers?

2. Methods

2.1. WRF-Modeling

In this study, we utilize version 4.4 of the Weather Research and Forecasting (WRF) model, which has been described in greater detail elsewhere (Parajuli et al., 2024, 2025). Briefly, the model setup includes three nested domains with horizontal resolutions of 9 km (d01), 3 km (d02), and 1 km (d03), as illustrated in Figure 1a. The finest-resolution domain, d03, encompasses all agricultural areas in the Imperial Valley and extends northward into the Coachella Valley. To more accurately capture heat exposure among farmworkers, many of whom commute daily from Mexicali, we also include Mexicali and its surrounding region within the model domain.

We use ERA5 data developed by European Centre for Medium-Range Weather Forecasts (ECMWF) as initial and boundary conditions, which is an hourly reanalysis data available at ∼31 km resolution (Hersbach et al., 2020). Convection is fully resolved in the finest domain (d03) while we parameterize convection in the two parent domains (d01, d02) using Grell and Freitas scheme (Grell & Freitas, 2014) (cu_physics = 3). Key modules used are Morrison double-moment microphysics scheme (Morrison et al., 2009), Yonsei University Scheme (YSU) planetary boundary layer scheme (Hong et al., 2006), Rapid Radiative Transfer Model (RRTMG) for both shortwave and longwave radiation (Iacono et al., 2008), and revised MM5 Monin-Obukhov surface layer scheme (Jiménez et al., 2012). We use the community Noah-MP land surface model (He et al., 2023) within WRF, which reproduces the hydroclimate over the continental US well (Rasmussen et al., 2023). Irrigation is applied within Noah-MP based on an LAI threshold using the USDA county-level irrigation data (Valayamkunnath, 2019). The irrigation is applied using the sprinkler irrigation option until the soil moisture reaches the field capacity, which is the default setting.

The WRF model results used in this study were previously validated against a set of observations (Figure 1b) (Parajuli et al., 2024). The validation shows that the model performs well in simulating the meteorological inputs as well the WBGT parameters. Inclusion of irrigation also significantly reduces the bias in humidity and air temperature. The use of reanalysis data (ERA5) as initial and boundary conditions, the high-resolution (1-km spatial resolution) model configuration, and the application of grid nudging resulted in robust simulations of the meteorological parameters that feed into WBGT.

The only difference between this study and our previous work (Parajuli et al., 2024) is the method used to calculate WBGT. In the previous study (Parajuli et al., 2024), we computed WBGT using the Thermofeel Python library (Brimicombe et al., 2022). Here, and in our another preceding study (Parajuli et al., 2025), we apply Liljegren's method (Liljegren et al., 2008) as implemented in PyWBGT (Kong & Huber, 2022), because Liljegren's method is generally considered more robust for WBGT estimation. All other aspects of the modeling framework remain unchanged. Specifically, the WRF model configuration and input parameters are the same, which have been previously validated (Parajuli et al., 2024).

2.2. WBGT Calculations

In this study, WBGT is calculated using the gold standard method (Kong & Huber, 2022), which can compute WBGT using meteorological observations or climate model outputs. Originally written in the C programming language, the method was recently implemented in Python as the PyWBGT package (Kong & Huber, 2022). Kong and Huber (2022) extended the method to calculate natural WBT and BGT to use longwave radiation (Tnwb_GCM and Tg_GCM). We evaluated the results using these updated equations against our field measurements of BGT (Parajuli et al., 2024) and found that Tg_GCM slightly improves the prediction of BGT compared to the original formulation (Tg_Liljegren) (Figure S2 in Supporting Information S1). Measured WBT data were unavailable so we were unable to compare the natural WBTs (Tnwb_Liljegren and Tnwb_GCM) but the demonstrated improvement in BGT alone provides justification to use WBGT_GCM. Therefore, we use WBGT_GCM in all of our calculations.

The inputs required for WBGT calculation include DBT, relative humidity, surface pressure, 2- or 10-m wind speed, surface downward and upward solar radiation, surface downward and upward longwave radiation, solar zenith angle, and the fraction of direct horizontal solar irradiance to the total horizontal solar irradiance. WBGT can be calculated using the above-mentioned method (Kong & Huber, 2022) as:

$$\begin{aligned}&\mathrm{WBGT\_GCM\_k} = \mathrm{xr.apply\_ufunc}\big(\mathrm{WBGT\_GCM, t2\_k, rh, psfc, va, swdnb, swupb,}\\&\mathrm{lwdnb, lwupb, f, czda, False, output\_dtypes} = [\mathrm{float}]\big)\end{aligned} \tag{2}$$

The description of the above input parameters and the corresponding WRF output variables are provided in Table 1.

2.3. WBGT Thresholds

General WBGT thresholds are recommended by National Weather Service (NWS) (NWS, 2023), which start at 80°F. Occupational WBGT thresholds are recommended by the National Institute for Occupational Safety and Health (NIOSH) (Jacklitsch et al., 2016), the American Conference of Governmental Hygienists (ACGIH) (ACGIH, 2017), and the US Army (DOA, 2003). In this study, the NWS WBGT categories beginning at 80°F are used as a regional heat-risk screening framework to describe the timing, frequency, and spatial pattern of heat threshold exceedance. Occupational heat stress is interpreted separately using the ACGIH/NIOSH framework, specifically the Recommended Alert Limit (RAL) and Recommended Exposure Limit (REL), which account for workload, acclimatization status, and clothing adjustment.

Heat stress experienced by a worker for a given WBGT depends upon clothing and level of physical activity or metabolic rate. For example, a person involved in heavy work activity will experience heat stress at lower WBGT compared to the worker involved in light work activity. Similarly, heat stress experienced by the worker increases significantly if the worker is wearing double or more layers of clothing. ACGIH (ACGIH, 2017)/NIOSH (Jacklitsch et al., 2016) recommends using effective WBGT ($WBGT_{eff}$) to account for the effect of metabolic heat and clothing. Workers typically wear double-layered clothing in the study area, therefore, we use NIOSH recommended clothing adjustment factor of 3°C (NIOSH, Table 3-2) for double-layered clothing and increase our model-calculated WBGT values uniformly by 3°C (5.4°F) to account for clothing effect. Unless otherwise mentioned, WBGT in this work refers to $WBGT_{eff}$.

Table 1
Inputs to Calculate WBGT (Kong & Huber, 2022; Liljegren et al., 2008) and Their Equivalent WRF Model Outputs

Parameters	Liljegren/PyWBGT input variables	Equivalent WRF output variable name	Remarks
Air temperature at 2 m	t2_k (K)	T2 (K)	Standard wrf output
Relative humidity at 2 m	rh (%)	rh_2m (%)	Calculated with the NCAR NCL script wrfout_to_cf
Surface pressure	psfc (Pa)	PSFC Surface pressure (Pa)	Standard wrf output
Wind speed at 10 m height	va (m s^{-1})	WS (m s^{-1}) $= \sqrt{(U10^2 + V10^2)}$	Calculated from standard WRF output $U10$ and $V10$
Cosine of solar zenith angle	Czda	COSZEN cosine of solar zenith angle	Standard wrf output
Total sky direct solar radiation at surface (downward on a horizontal plane)	–	SWDDIR Shortwave surface downward direct irradiance (W m^{-2})	Not a standard WRF output, added in myoutfields.txt
Surface solar radiation downwards	swdnb (W m^{-2})	SWDOWN (W m^{-2}) downward short-wave flux at ground surface	Standard wrf output
Ratio of direct horizontal solar irradiance to the total horizontal solar irradiance	F	SWDDIR/SWDOWN	–
Surface solar radiation upwards	swupb (W m^{-2})	SWUPB (W m^{-2}) instantaneous upwelling shortwave flux at bottom	Standard wrf output
Surface thermal radiation downwards	lwdnb (W m^{-2})	GLW (W m^{-2}) downward long wave flux at ground surface	Standard wrf output
Surface thermal radiation upwards	lwupb (W m^{-2})	LWUPB (W m^{-2}) instantaneous upwelling longwave flux at bottom	Standard wrf output

NIOSH recommends using different thresholds for unacclimatized and acclimatized workers to account for the effect of metabolic heat, given by RAL and REL, respectively, as per the following equations:

$$\mathrm{RAL(WBGT)} = 59.9 - 14.1\ \log_{10} M \tag{3}$$

$$\mathrm{REL(WBGT)} = 56.7 - 11.5 \log_{10} M \tag{4}$$

The total heat exposure for unacclimatized and acclimatized workers should be controlled so that workers are not exposed to combinations of metabolic and environmental heat greater than the applicable RAL and REL (Jacklitsch et al., 2016).

2.4. Heat Exposure by Crop Types

Heat exposure across different crop types was determined by averaging the $\mathrm{WBGT_{eff}}$ over the crop harvest work shifts and calendar months considering reference metabolic rates. The work hours and harvest month information (Table 2) were compiled from multiple sources including direct interviews and field surveys together with data from Imperial County Farm Bureau (ICFB, 2024). We conducted several meetings with representatives from the farmworker advocacy organization Líderes Campesinas to identify crop-specific seasonality and typical shift times for each crop. Líderes Campesinas representatives were also former farmworkers with direct experience working in regional agricultural work. Additionally, we drew from interviews and focus groups with 27 farmworkers and 9 peer managers (called "mayordomos") and shift times and corresponding crop types were cross checked from survey data with 300 farmworkers collected as part of our larger parent study. While there was some variation in shift hours, we determined typical shift hours by crop from qualitative assessment of all these data sources. Although we cannot capture variation across specific farms and years, we assume that the crop- and shift-specific exposure are broadly representative of the region.

The references used to estimate metabolic rate for different crops are provided in the table (Table 2) for each crop. Although these metabolic rates used correspond to different regions around the world, the physical activity associated with a crop should not be very different in different regions so it is reasonable to assume that metabolic rates are fixed for a crop type. For corn, melons, onions, and olives, we were unable to find the metabolic rates from the literature. So we used an indirect approach to estimate the metabolic energy spent by workers to work on

Table 2
Common Crops and Their Harvest Month/Hours in the ICV Region With Corresponding Estimated Metabolic Rates

Crop	Hours start-end	Months start-end	Metabolic rate range (W) (reference)	Labor category (as per ISO (ISO, 2017))	Land preparation/harvest time
Corn	1 a.m.–6 p.m.	August–October	244–310 (Pan et al., 2021)	Medium	Land preparation
Melon	6 a.m.–5 p.m.	May–June	231–293 (Pan et al., 2021)	Medium	Harvest
Onions-day	6 a.m.–2 p.m.	May–June	217–275 (Pan et al., 2021)	Medium	Harvest
Onions-night	6 p.m.–1 a.m.	May–June	217–275 (Pan et al., 2021)	Medium	Harvest
Grapes	5 a.m.–2 p.m.	April–June	258–327 (Poulianiti et al., 2019)	Medium	Harvest
Dates	5 a.m.–3 p.m.	August–September	200–260 (Mohammadian et al., 2020)	Medium	Harvest
Winter veggies (Lettuce/Carrots/Broccoli/Cauliflower/Kale)	6 a.m.–3 p.m.	June–September	146–181 (Carrots) (Edholm et al., 1973)	Light	Land preparation
Olives	5 a.m.–2 p.m.	September–October	285–361 (Pan et al., 2021)	Medium	Harvest
Cane	6 a.m.–2 p.m.	April–October	637–770 (Davies et al., 1976)	Very heavy	Harvest
Alfalfa/Sudangrass	6 a.m.–5 p.m.	January–December	–	–	Harvest and land preparation

these crops. A recent study estimated metabolic expenditure in terms of metabolic equivalents using an accelerometer among the farmworkers in the central and imperial valleys (Pan et al., 2021). Using the metabolic equivalents for these crops, and using "grapes" as reference for which metabolic rate is known (258–327 W) (Poulianiti et al., 2019), we estimated the metabolic rates for these crops by multiplying the grape's metabolic rate with the ratio of metabolic equivalents for a specific crop to that of grapes (1.9).

2.5. Critical Crop Zone Mapping

The critical crop zone map was developed by integrating modeled effective WBGT ($WBGT_{eff}$) data with crop maps from Land IQ, an initiative led by the California Department of Water Resources to produce a comprehensive spatial land use database for California (CDWR, 2020). We used the Water Year 2020 data set, which includes multi-crop field mapping for fields larger than 2 acres across the state, derived using a supervised random forest classification of satellite and aerial imagery. To identify critical crop zones, we calculated the average of daily maximum $WBGT_{eff}$ within selected crop polygons using bilinear interpolation of the WBGT data during key seasonal windows (April-May and June-July-August).

2.6. Productivity Loss Calculations

Axelson (1974) first provided a formulation to calculate productivity loss at high heat stress based on field data (Wyndham, 1969), measuring decrease in productivity at increasing effective temperatures for miners. Generally speaking, there are two most commonly referred labor response functions (LRFs) used to determine productivity loss due to heat stress. One is based on the adoption of work-rest cycles to avoid health risk (ISO-LRF) (Bröde et al., 2018; d'Ambrosio Alfano et al., 2014; Malchaire, 1979). Another is based on the empirical relationship between WBGT and measured labor productivity among mine workers in South Africa and rice harvesting workers in India defined as workability (Kjellstrom et al., 2009, 2014, 2018; Sahu et al., 2013). The ISO-LRF is more restrictive, providing 100% loss of productivity starting at WBGT ~33°C, while the empirical function is less restrictive and provides gradual loss of productivity up to 40°C (Figure S3 in Supporting Information S1).

We calculate modeled productivity loss using Kjellstrom's labor response function (LRF) as a function of WBGT, which is derived using measured data. Kjellstrom defined productivity in terms of "workability," which is obtained by the following equation (Bröde et al., 2018):

$$\text{Workability}_{\text{Kjellstrom}} = 0.1 + \frac{0.9}{\left\{1 + \left(\frac{\text{WBGT}}{\alpha 1}\right)^{\alpha 2}\right\}} \tag{5}$$

where ($\alpha 1$, $\alpha 2$) are constants with values (34.64, 22.72) for low (M = 180 W), (32.93, 17.81) for moderate (M = 300 W), and (30.94, 16.64) for high (M = 400 W) workload.

Since Kjellstrom's LRFs are available only for acclimatized workers, we derive LRFs for unacclimatized workers with the aid of another method which is used by International Organization for Standardization (ISO-LRF) as follows:

$$\text{Workability}_{\text{ISO}} = \max\left[0;\ \min\left[1;\ \frac{\text{WBGT}_{\text{lim,rest}} - \text{WBGT}}{\text{WBGT}_{\text{lim,rest}} - \text{WBGT}_{\text{lim}}}\right]\right] \tag{6}$$

Where, WBGT_{lim} is calculated separately for unacclimatized (RAL) and acclimatized workers (REL) from ISO/NIOSH guidelines as,

$$\text{RAL}(\text{WBGT}_{\text{lim}}) = 59.9 - 14.1 \log_{10} M \tag{7}$$

$$\text{REL}(\text{WBGT}_{\text{lim}}) = 56.7 - 11.5 \log_{10} M \tag{8}$$

and $\text{WBGT}_{\text{lim,rest}}$ for the acclimatized and unacclimatized workers is obtained by using metabolic rate at rest (M = 117 W) in Equations 7 and 8, respectively.

The ISO-LRFs for acclimatized and unacclimatized workers at different metabolic rates are parallel, that is, for unacclimatized workers, the same amount of labor capacity is reached earlier at an average of 2.42°C lower WBGT than for acclimatized workers (Figure S3 in Supporting Information S1). With this assumption, we calculated the workability for unacclimatized workers using the same Equation 5 but by increasing the WBGT values by 2.42°C (note the inverse relationship between workability and WBGT in Equation 5).

Since workability or work capacity is defined as the percentage of a working hour that a worker can safely perform, we present our results in terms of modeled productivity loss given as:

$$\text{Modeled productivity loss} = \left(1 - \text{Workability}_{\text{Kjellstrom}}\right) \times 100 \tag{9}$$

Using the simulated hourly WBGT, we first calculated hourly workability from the Kjellstrom labor response function (LRF) (Equation 5) and then converted it to productivity loss using Equation 9. Therefore, in this study, modeled productivity loss is an LRF-based estimate of heat-related reduction in work capacity embedded in the published WBGT–workability relationship, and it is not an explicit simulation of mandated rest periods, regulatory compliance, or worker behavioral adaptation. We then computed shift-mean modeled productivity loss for three work shifts (9 a.m.–5 p.m., 4 a.m.–12 p.m., and 4–12 p.m.) by averaging hourly modeled productivity loss across the hours in each shift, spatially averaged over the Imperial Valley bounding box (Figure 1a), and summarized by month. Modeled productivity loss varies by work shift and month because WBGT differs across shifts and seasons. A Python notebook provided in the GitHub data repository documents the full procedure used to calculate labor productivity in this study.

3. Results

3.1. Exceedance of Heat Stress Thresholds (WBGT)

The WBGT_{eff} (WBGT with clothing correction; see Methods) hourly exceedance varies greatly with season, with maximum exceedance in the summer months during both day and night (Figure 2). For the year 2020, August has the highest number of hours when WBGT_{eff} exceeds the critical threshold of 80°F recommended by NWS

10.1029/2025GH001604

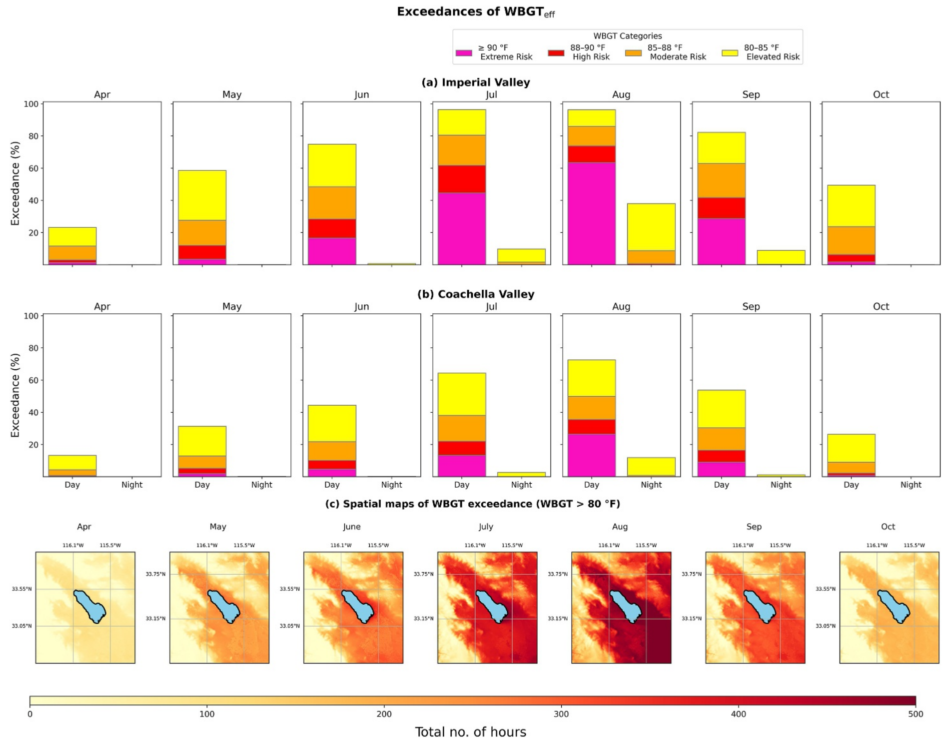

Figure 2. Hourly exceedances (%) of $WBGT_{eff}$ by day and night between April and October (2020) for (a) Imperial Valley and (b) Coachella Valley, within the bounding boxes in Figure 1. "Day" represents hours from 7 a.m. to 7 p.m. and "night" represents 7 p.m.–7 a.m. (c) Maps of total exceedance hours (WBGT > 80°F) in different months.

(NWS, 2023). In the Imperial Valley, this happens 96.3% of the time during the day and 38.0% at night (Figure 2a). In the Coachella Valley, it happens 72.5% during the day and 11.9% at night (Figure 2b).

$WBGT_{eff}$ reaches even the highest category (>90°F) in all months (April-Oct) except April in the Imperial Valley. The $WBGT_{eff}$ threshold of 80°F is exceeded during the major harvesting months April, May, September, and October in the daytime. In April, $WBGT_{eff}$ exceeded 80°F 23.2% of the time during the day in the Imperial Valley and 13.2% of the time in Coachella Valley. Nighttime exceedances are considerable in summer months but negligible in the harvesting months. Exceedance rates are lower in the Coachella Valley compared to the Imperial Valley, which can be explained by the generally cooler weather in Coachella Valley lying north of the Imperial Valley. The pattern of exceedance is spatially uniform across the ICV region in a given month (Figure 2c). The total number of hours exceeding 80°F reaches more than 500 in August, with considerable exceedances in all harvesting months.

$WBGT_{eff}$ varies across seasons, hours, and crop types (Figure 3). Hours shaded in pink (first panel) indicate potentially unsafe conditions where caution is advised, whereas blue or white represent safer windows for outdoor labor. $WBGT_{eff}$ reaches high values even during the evenings and early mornings, as indicated by pink colors in Figure 3. The second panel shows the same diurnal variation but using standard WBGT categories in practice, in which different precautionary measures are recommended for different categories (Table S1 in Supporting Information S1). $WBGT_{eff}$ exceeds even the highest category (>90°F) during several hours of the day between May to September (Figure 3b). $WBGT_{eff}$ returns to the safe level (<80°F) typically after 6 p.m. until 7 a.m. in the morning in most of the months except August.

3.2. Heat Exposure by Crop Types

Contrary to the expectation that many work shifts would occur at night during hotter months, most work shifts start between 5 and 6 a.m. and end between 1 and 3 p.m. (Table 2), which includes the hottest part of the day. Only onions were reported to be harvested at night. $WBGT_{eff}$ varies substantially across crop types due to differences in typical work hours and harvest seasons (Figures 3 and 4). The critical threshold of 80°F is exceeded for at least

10.1029/2025GH001604

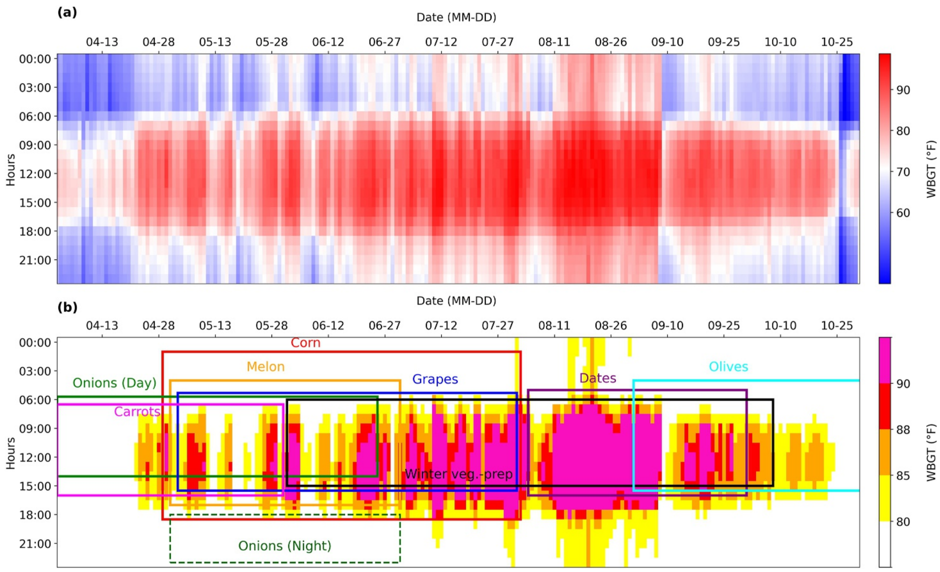

Figure 3. Variation of $WBGT_{eff}$ across hours and seasons. (a) Hourly heatmap of $WBGT_{eff}$ during the warm (April–October) months. (b) Same as (a) but using commonly used WBGT categories with harvest window (hours and months) for major crops. Data are averaged over the IV region (Figure 1, blue box).

part of the work shift for most crops (Figure 3), indicating potential heat stress risk in all crop categories except for onions harvested at night. The $WBGT_{eff}$ of several crops exceeds the highest safety threshold (95°F) during part or a majority of the shift. Dates are the crop with the highest average $WBGT_{eff}$ during work periods (Figure 4), as they are primarily harvested during daytime hours in the hottest summer months. Nighttime harvesting of dates is not feasible due to safety concerns involving the use of ladders and artificial lighting (Mayer, 2023). Land preparation for winter vegetables has high $WBGT_{eff}$ because it also happens during the day in summer.

The spatial distribution of crop fields, together with $WBGT_{eff}$ averaged within the crop-specific harvest windows, shows that fields with high heat exposure are widespread but also show clustering (Figure 5). In the Imperial Valley, all crops fall into the moderate-risk category (85°F < $WBGT_{eff}$ < 88°F) during the spring harvest months. According to NWS recommendations (Table S1 in Supporting Information S1), farmworkers in these zones should take 30-min rest breaks per work hour when working in direct sunlight, with appropriate adjustments based on work shift, season, and acclimatization status (Parajuli et al., 2025). In the Coachella Valley, $WBGT_{eff}$ reaches the high-risk category (88°F < $WBGT_{eff}$ < 90°F) in some fields for crops such as grapes, melons, and onions, while the remaining crop zones remain in the moderate-risk category, indicating elevated heat exposure. Crop diversity is greater in the Imperial Valley, with dominant crops including alfalfa, corn, sudangrass, melons,

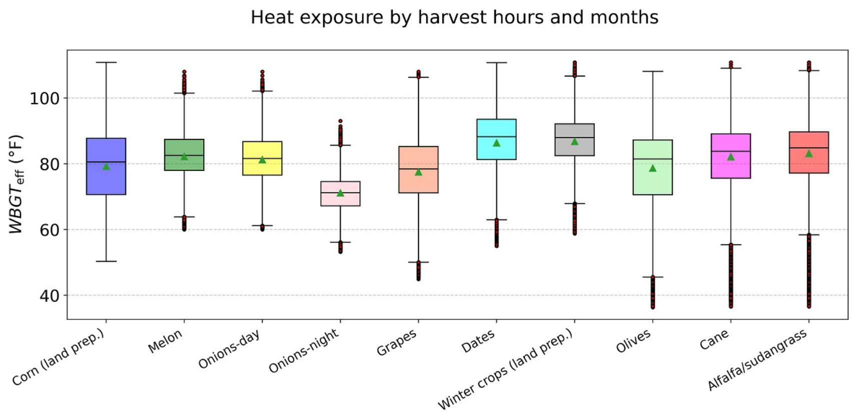

Figure 4. Boxplot of $WBGT_{eff}$ by crop type based on the crop-specific work windows (Table 2 and Figure 3). For corn and winter crops, land preparation time is used instead of the harvest window.

10.1029/2025GH001604

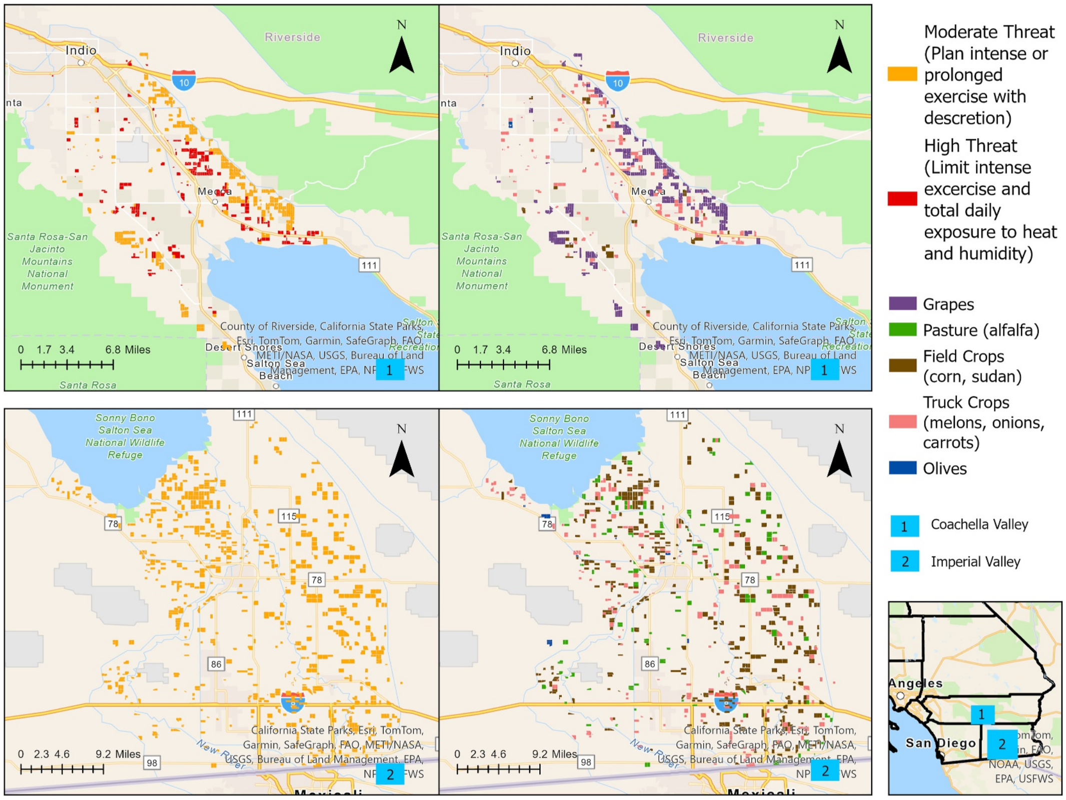

Figure 5. Maps of critical crop zones with high heat exposure. $WBGT_{eff}$ categories (left panels) for major crop types (right panel) in (1) Coachella (2) Imperial Valley, averaged during spring harvest season (April–May).

onions, and carrots, whereas the Coachella Valley shows lower diversity, dominated primarily by grapes and dates (Figure 5 and Figure S1 in Supporting Information S1). High heat-risk conditions persist into summer in the Coachella Valley with major harvests of grapes and dates, whereas the Imperial Valley shows more limited crop activity during summer months (Figure S1 in Supporting Information S1).

Including crop-specific metabolic expenditure and acclimatization (ACGIH, 2017; Jacklitsch et al., 2016) highlights additional risks for heat exposure (Figure 6). For all crops, except onions harvested at night, $WBGT_{eff}$ exceeds the Recommended Alert Limit (RAL) for unacclimatized workers. In the case of dates and sugarcane, $WBGT_{eff}$ even surpasses the Recommended Exposure Limit (REL), meaning that work on crops may be unsafe or requires additional protective measures such as rest breaks even for acclimatized workers (Parajuli et al., 2025). Sugarcane harvesting, in particular, involves high-intensity tasks such as bending, cutting, and lifting, resulting in elevated metabolic demands and increased heat stress risk. These results indicate a clear need to adjust harvest hours or take precautions otherwise, particularly for high-risk crops, to reduce worker exposure and maintain conditions within safe occupational heat thresholds.

3.3. Irrigation Impact on Heat Thresholds

Irrigation, as simulated by our model (Parajuli et al., 2024), impacts the WBGT differently during the day as compared to night, with up to 2.5°F reduction in the daytime, but a similar increase at night (Figure 7a). At night, while most grid cells in the IV region exhibit WBGT values below 80°F, a substantial number exceed this threshold even without irrigation (Figure 7b). Grid cells with WBGT values near 80°F are particularly sensitive; for instance, nighttime WBGTs in the 79–83°F range can increase by up to ~0.75°F by irrigation, often crossing the 80°F threshold. In contrast, daytime irrigation generally reduces WBGT, as indicated by the predominance of values below the zero line. This cooling effect is most pronounced in the higher WBGT range (~90–93°F), suggesting that irrigation is beneficial for mitigating high heat stress during the day. The times when the irrigation

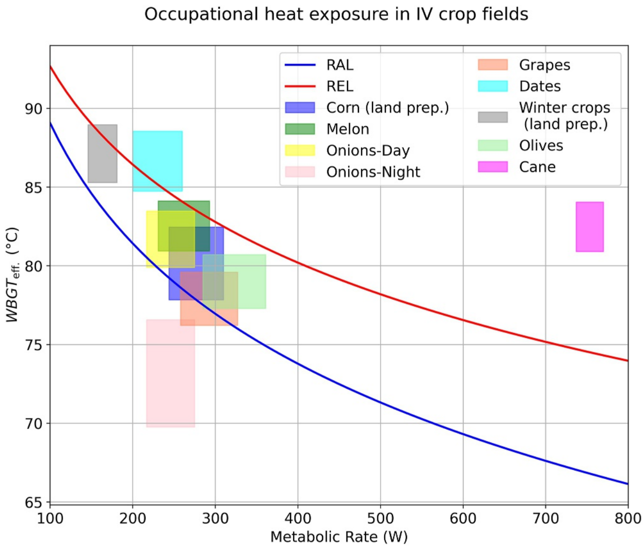

Figure 6. Crop-specific occupational heat stress exceedance for different months based on ACGIH (ACGIH, 2017)/NIOSH (Jacklitsch et al., 2016) threshold limits. The $WBGT_{eff}$ range represents the average $WBGT_{eff}$ within IV crop fields (Figure 1, blue box). The range of metabolic rates for different crop types are obtained from Table 2. Recommended Alert Limit (RAL) and Recommended Exposure Limit (REL) represent WBGT thresholds for unacclimatized and acclimatized workers. For corn and winter crops, the land preparation period is used instead of the harvest window.

effect shifts from positive to negative or vice versa (around 07:30 and 17:00) are particularly noteworthy (red dotted lines, Figure 7c).

3.4. Heat Exposure During Heatwaves

A total of 158 heatwave days were identified in the Imperial Valley in 2020 using an agricultural station as a reference (Seeley), defined by periods where daily maximum temperatures exceeded 95°F for at least five consecutive days (Collins et al., 2000) (Figure 8a). This highlights a severe and prolonged heat risk for farmworkers in the study region, as some crop-related activities such as harvesting, land preparation, and irrigation setup occur throughout all warm-season months. The California Code of Regulations (CCR) (CCR, 2005) defines heatwave days as the days in which daily maximum temperatures exceed 80°F and is at least 10°F higher than the average during the preceding 5 days. The CCR definition identifies substantially fewer heatwave days compared to our calculation using the 95°F threshold sustained over five consecutive days. Only 9 heatwave days were identified in 2020 using the CCR method (Figure 8b). Notably, most of these CCR-identified events occurred during the cooler shoulder seasons (April–June and October–November), rather than in the core summer months when heat-related health risks are highest. This is because in desert regions such as the IV, temperature rises gradually and remains high for several days, but abrupt increases in temperature by 10°F might be rare. This seasonal misalignment suggests that the CCR criteria may fail to detect many hazardous periods of extreme heat. By contrast, the proposed 95°F threshold more effectively captures prolonged periods of elevated temperatures from April to October, offering a more realistic detection of heatwaves. We used one representative station (Seeley) for identifying the heat waves because heat waves typically cover a large region, all showing a similar trend.

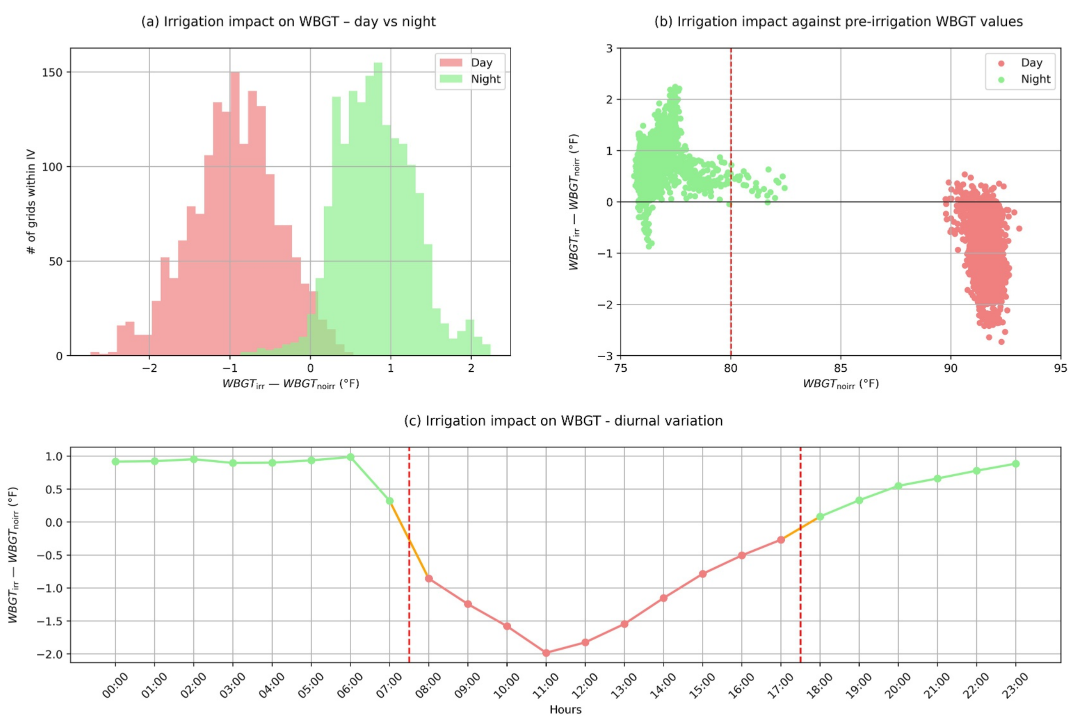

Figure 7. Irrigation impact on WBGT. (a) Histograms of WBGT difference between irrigation-on and irrigation-off WRF runs for the grids within IV region, shown separately for day and night for August 2020. (b) WBGT difference plotted against pre-irrigation WBGT. (c) Diurnal variation of the irrigation effect on WBGT.

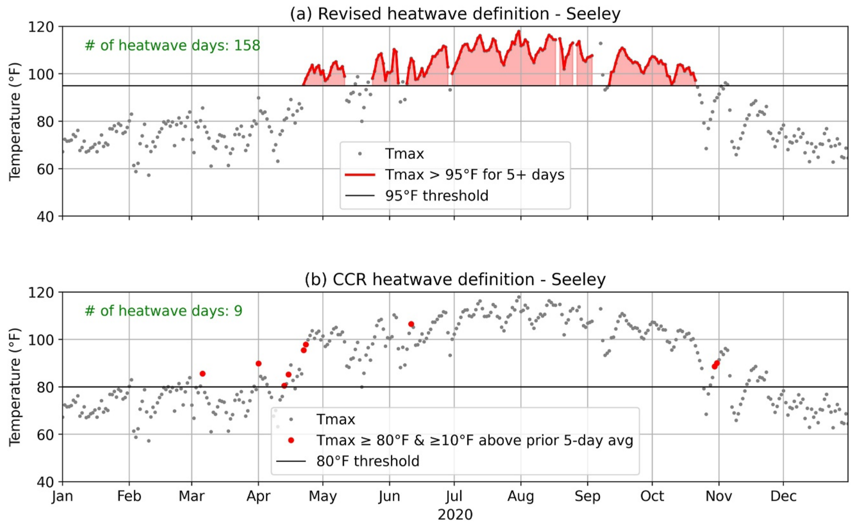

Figure 8. Heatwave events of 2020 in the Imperial Valley were identified with a reference station Seeley, based on (a) modified heatwave definition (daily maximum temperatures exceeding 95°F for 5 or more consecutive days) (b) California Code of Regulation definition of heatwaves.

During the most intense heatwave of 2020 (July–August), the daily maximum 2-m air temperature rose to nearly 120°F in the Imperial Valley (Figure 9a). The nighttime minimum temperature fell below 80°F, allowing some recovery from heat for residents. Relative humidity remained below 40% during most of the heatwave, with an exceptional spike on the night of August 01 (Figure 9b), which is caused by increased evaporation from the Salton Sea (Parajuli et al., 2024). This spike raised the daily minimum WBGT at night by ∼ 4°F (Figure 9d). The upwelling longwave radiation notably increased due to strong heating of the land surface during the heatwave (Figure 9c), which worsens heat stress by increasing the black globe temperature, a component of WBGT. The WBGT during the heatwave reached above 95°F, while remaining above the critical threshold of 80°F for several hours at night (Figure 9d).

3.5. Impact on Labor Productivity

Modeled productivity loss also varies across hours and seasons due to variation in heat exposure (Figure 10). Maximum modeled productivity loss occurs for unacclimatized workers performing heavy work (Figure 10a), while it is minimum for acclimatized workers performing light work (Figure 10b). The maximum modeled productivity loss exceeds ∼80% during the summer months. The modeled productivity loss for acclimatized workers performing light work exceeds ∼50% in the summer, while it remains lower during the remaining periods. There is a notable variation in modeled productivity loss across hours, suggesting that heat exposure, and consequently productivity loss, clearly depends on the work hours.

Modeled productivity loss increases with the progression of warm months, reaching its highest in August. Three scenarios involving different work shifts are presented, depicting variation in modeled productivity loss across shifts. Modeled productivity loss exceeds 55% in August for the baseline work shift (9 a.m.–5 p.m.). The modeled productivity loss is reduced to below 25% in the early morning shift (4 a.m.–12 p.m.) and below 15% in the evening shift (4 p.m.–12 a.m.). These results suggest that productivity loss can be significantly reduced, by up to 40%, by adjusting the work schedule. Adoption of evening shift may be preferable for reducing heat exposure as it results in lowest productivity loss although the morning shift also reduces productivity loss remarkably.

As per the county-level farm employment database (CES, 2020), maximum farm employment is observed in May in Imperial County, with over 12,000 workers, indicative of the peak harvesting month. Farm employment in Imperial County suddenly drops with the start of summer (∼25%) to a base level of ∼9,000 workers (Figure 11b) with no further reduction in the following months. This trend in farm labor deployment likely reflects a seasonal reduction in crop harvesting activities and, as a result, may also reduce overall heat exposure across the worker population. During the peak labor deployment month (May), there is considerable daytime WBGT exceedance across all WBGT categories, with no remarkable exceedance at night (Figure 2). This employment pattern may

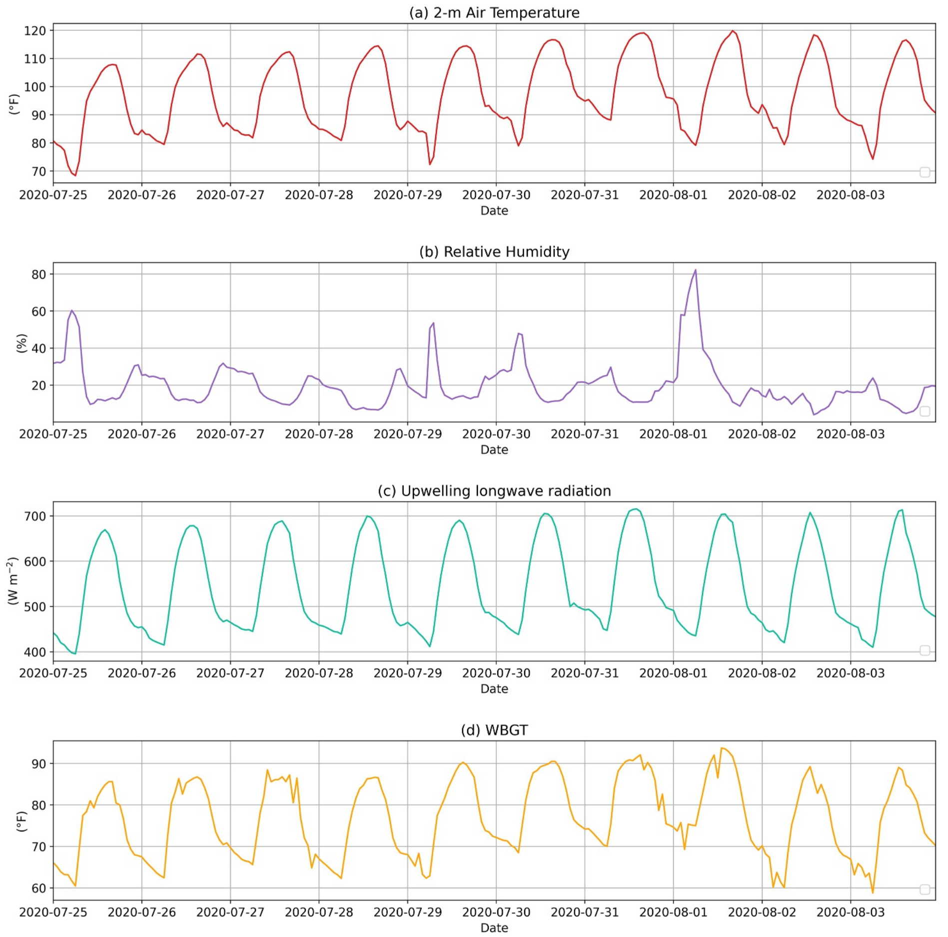

Figure 9. Time series of heat stress parameters at Seeley (Imperial Valley) during the most intense heatwave of 2020. (a) 2-m air temperature, (b) relative humidity, (c) upwelling longwave radiation, and (d) WBGT.

also have implications for labor productivity because fewer workers are employed during the hottest months (July–September), when heat stress and associated productivity loss are highest (Figure 11a), while more workers are employed during relatively cooler months (April-May) when productivity losses are lower.

4. Discussion and Summary

The farmworkers in the ICV region face unique heat-related challenges. Many already endure difficult working conditions and are exposed to heightened heat risk during planting and harvesting periods. Our study estimates the heat exposure among the farmworkers in the ICV crop environments using hourly outputs from a high-resolution (1-km grid) regional weather forecasting model (WRF). We used hourly WBGT estimates by crop type to estimate when conditions exceed recommended heat stress thresholds. These thresholds are based on guidelines from the American Conference of Governmental Industrial Hygienists (ACGIH®) (ACGIH, 2017) and the National Institute for Occupational Safety and Health (NIOSH) (Jacklitsch et al., 2016), which consider factors including clothing and different work load conditions. Heat stress is often quantified using simplified indices like Wet Bulb Temperature (WBT) or simplified WBGT because global general circulation models often lack key inputs like radiation (Chakraborty et al., 2022; Vecellio et al., 2023; Zhao et al., 2021). Our WBGT exceedance calculations are based on the gold-standard Liljegren method (Kong & Huber, 2022; Liljegren et al., 2008), which includes key contributors of heat stress, including humidity as well as longwave and shortwave radiation, and thus provides a much more accurate assessment of field-level heat exposure on farmworkers.

Our analysis shows that heat exposure has a strong diurnal cycle but also varies by crop type. The recommended occupational WBGT threshold (80°F) is frequently exceeded even in the cooler harvesting seasons (April-May,

10.1029/2025GH001604

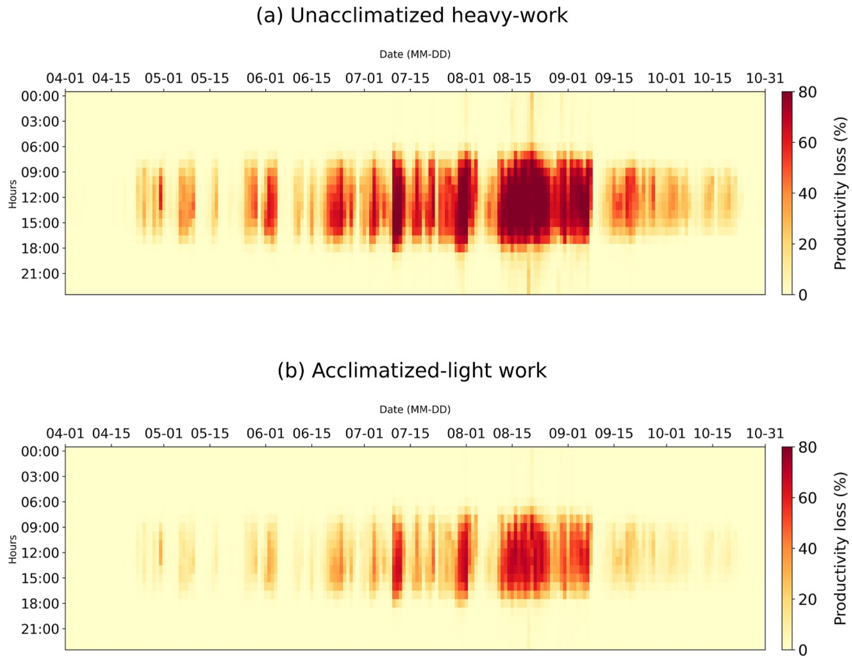

Figure 10. Modeled heat-related productivity loss (%) by hours of the day for unacclimatized and acclimatized farmworkers averaged within the Imperial Valley, during the warm months (2020).

September-October), ranging from 100 to over 500 hr in different months. Even the highest WBGT category (>90°F) is exceeded for considerable work hours in most harvesting months. Urban areas such as El Centro and Mexicali have many more exceedance hours compared to the agricultural crop fields due to urban heat island effects. Existing evidence shows that nearly all heat-related illness incidents and fatalities occur when $WBGT_{eff}$ exceeds occupational limits (Morris et al., 2019). The large number of annual heatwave days (158), some of which also fall within key harvesting months (May and October), indicates that the ICV region is a high heat-risk environment for farmworkers.

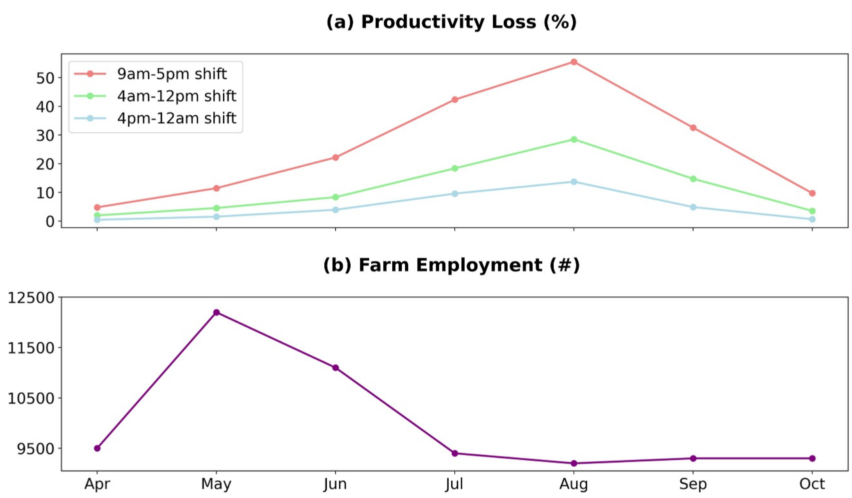

Figure 11. Modeled heat-related labor productivity loss by work shift. (a) Modeled productivity loss based on WBGT averaged by month within the IV crop fields (Figure 1). (b) No. of farm employment in Imperial County. Both data are for April–October 2020.

4.1. Policy Implications

Our comprehensive results on heat exposure, examining its variation across hours, seasons, and crops, allow us to propose a number of mitigation measures to reduce the heat exposure among farmworkers in the ICV region as discussed below. However, because we did not use any health outcome data in this study, the following mitigation measures should only be interpreted as inferential recommendations, which require confirmation through future health, behavioral, and implementation research.

4.1.1. Adjusting Outdoor Work Hours

One immediate strategy to reduce heat exposure is changing the timing of work shifts. Our results show that heat stress exceedance has a clear diurnal variation (Figure 3). Therefore, altering work shifts even by a few hours to utilize cooler morning or evening hours can significantly reduce heat exposure. In fact, some farmworkers mentioned that such adjustments in work shifts are already in practice in the region in high-heat periods during the summer, although regulations do not formally recognize this. The effectiveness of such practice is evident from our results, but we note that commonly-practiced work shifts in the ICV region still include the hottest hours of the day carrying substantial heat risks. Our results showed that shifting the work hours to an early morning or late evening shift can reduce the productivity loss by up to 30% and 40%, respectively, while also protecting workers from extreme heat. While working at nighttime is becoming more common in some places (Mayer, 2023), adjusting work hours must account for constraints such as child care, sleep schedule disruption and safety concerns.

4.1.2. Use of WBGT Instead of Air Temperature

Current heat protection regulations in California, such as California Code of Regulations (CCR) T8 §3395 [60], rely on air temperature to specify protective measures in high-heat conditions. For example, CCR requires employers to provide access to shade when the air temperature exceeds 80°F threshold and provide 10-min rest breaks every two hours when the air temperature exceeds 95°F. But air temperature alone can misrepresent actual heat risks because this single metric does not consider the specific impact of solar radiation, wind speed, and humidity, which are key factors in the ICV agricultural fields. The WBGT thresholds have been linked to observed health risks and can provide a better measure of heat exposure (ISO, 2017; Jacklitsch et al., 2016), even though WBGT values are less intuitive and appear lower than air temperature. WBGT monitoring remains rare among farmworkers, likely due to equipment costs and logistics. In this context, a regional forecasting approach can address current gaps in early warning systems at city or farm-level scales (Vargo et al., 2015). Although simplified WBGT metrics have been widely used (Bernard & Barrow, 2013; Clark & Konrad, 2024), our work suggests that a more rigorous monitoring of WBGT in combination with a weather model is both feasible and effective in agricultural settings.

4.1.3. Adopting Variable Rest-Break Schedule

Heat exposure among farmworkers varies with season, work shift, crop type, and level of acclimatization. Therefore, rest-break needs also vary accordingly in different work settings (Parajuli et al., 2025). As a result, fixed rest-break durations specified in CCR may not provide adequate protection across diverse work settings. Tailoring rest-breaks to the specific conditions can help minimize heat risk. Clearer and more detailed rest-break guidelines in CCR and related resources would support employers in implementing more protective schedules for farmworkers.

4.1.4. Reducing Nighttime Heat Exposure

WBGT thresholds are exceeded frequently, even in the nighttime, in the ICV crop fields. Certain crops are harvested at night, for example, onions, so the nighttime heat exposure should also be considered during summer, although our results show that nighttime harvesting during the spring season appears safe. Additionally, as many of the workers also live in the cities in the agricultural region, nighttime heat continues to affect the workers at their homes. Without nighttime cooling, particularly in homes without AC, workers may not recover properly, which increases their vulnerability to heat stress the following day. Many farmworkers live in the ICV city areas, often in homes without air conditioning (Kamai et al., 2023). A recent study found that nighttime heat is more related to preterm childbirth than daytime heat (Ward et al., 2019). Therefore, new policies should consider these off-hours risks and encourage nighttime cooling strategies, such as access to public cooling centers, home retrofits, or subsidies for air conditioning.

4.1.5. Avoiding Nighttime Irrigation

Our results showed that irrigation may increase WBGT at night. In areas where WBGT is close to 80°F, nighttime irrigation can cause WBGT increases of ∼0.75°F, enough to cross the critical heat stress threshold. The irrigation impact on WBGT is minimal during early morning or late afternoon transitional periods (around 07:30 and 17:00). Therefore, these transitional windows may be considered ideal for scheduling irrigation. While daytime irrigation provides a net cooling effect on WBGT, it results in higher evaporative losses, which is not desired from a water conservation perspective.

4.1.6. Identifying and Mapping High-Risk Crops

Dates and sugarcane are associated with extreme heat exposure due to their peak harvest occurring during the hottest hours/months and the intense physical labor required for their harvest (Figure 6). Therefore, it is important to identify these critical crop zones and provide extra precautions for the workers in these fields. The spatial identification of high-risk crops and their associated microclimates allows for a more targeted intervention strategy. Our critical crop zone map (Figure 5) can be used to prioritize resource allocation, such as water access points, mobile shade structures, and targeted heat warnings. Alternation of work schedule is highly recommended in these crop zones to minimize heat exposure (Parajuli et al., 2025).

4.1.7. Revising Heat Thresholds

Our results show that California's current heatwave definition (CCR), which is based on a comparison of daily highs to the five preceding days, fails to capture major heat events in already hot regions like the ICV region (Figure 8). In the desert environments such as the ICV, the daily maximum temperature rises gradually over several weeks, and the most dangerous conditions occur when the CCR method does not detect significant change due to uniformly high temperature and low deviation from the mean. We proposed and compared the effectiveness of a simpler definition of heatwaves: defined as five or more consecutive days exceeding 95°F (Collins et al., 2000). This revised definition aligns with international standards (e.g., WMO) (WMO, 2016) and uses the same threshold adopted by CCR to recommend high heat procedures, not to define heatwaves (CCR, 2005). For cooler regions such as coastal areas, the 95°F threshold can be adjusted downward. While this simple definition identifies the major heat waves, a health-based approach using heat-related illness and mortality data should be used to refine heatwave definitions, although such analysis is beyond the scope of this study.

4.1.8. Limitations

High-resolution regional simulations are typically used for localized, fine-scale analysis because of their high computational cost. Therefore, we conducted simulations for only one representative year, 2020, in this study. To evaluate sensitivity to interannual variability, we repeated the exceedance analysis for a second recent year (2024) using the same configuration and methods. We chose 2024 for the additional sensitivity analysis because it was the most recent year with complete data availability at the time the study was conducted. During the cooler harvest period (April), the exceedance of $WBGT_{eff}$ > 80°F is stable across years for both day and night. April daytime exceedance is nearly identical in 2020 and 2024 (Imperial Valley 23.2% vs. 23.6%; Coachella Valley 13.2% vs. 13.1%), while April nighttime exceedance is negligible in both years and both valleys. In contrast, the summer period (August) shows stronger interannual variability. August daytime exceedance remains high but differs substantially between years (Imperial Valley 96.3% vs. 82.3%; Coachella Valley 72.5% vs. 60.8%), and August nighttime exceedance also varies markedly (Imperial Valley 38.0% vs. 21.5%; Coachella Valley 11.9% vs. 7.9%). These results support the robustness of the main conclusions regarding seasonal contrasts and regional differences in heat risk, while indicating that the magnitude of summer exceedance, especially at night, should be interpreted cautiously when using a single year. Future studies should evaluate crop-specific WBGT exceedances using a multi-year climatology (Thompson et al., 2025) to better assess the generalizability of these findings.

Our results are derived from coarse-resolution simulations at 1-km spatial resolution, which may have some biases (Parajuli et al., 2024) that could influence the exceedance of the thresholds. The metabolic rates assumed in this study were derived from other regions, which may not accurately reflect the level of work activity in the ICV fields. The modeled productivity loss is calculated using an empirical function developed using limited data from another region (Kjellstrom et al., 2009, 2014, 2018; Sahu et al., 2013), which may not also accurately reflect the labor response profile in the ICV region. Another limitation of our study is the exclusion of air pollution impact on heat stress. Research from California's Central Valley has shown that ozone exposure also reduces farmworker productivity (Graff Zivin & Neidell, 2012). Future studies should integrate air quality data with heat exposure modeling to provide a more comprehensive view of environmental stressors. We also did not consider the actual health impacts using heat-related illness and mortality data while calculating heat exposure. Future studies should evaluate the WBGT exceedances and heat thresholds using health data to know whether the exceedances align with timing of health events and/or labor activities. Finally, the irrigation effect presented here is based on idealized irrigation using a model and does not represent observed farm-level irrigation practices. In reality, the irrigation response is likely to vary by crop type, irrigation method, and irrigation timing. Future work should quantify how this effect changes across crops, seasons, and actual irrigation schedules in the study area.

Conflict of Interest

The authors declare no conflicts of interest relevant to this study.

Availability Statement

ERA5 surface and pressure-level data used for driving WRF model were obtained from the Copernicus Climate Data Store (Hersbach et al., 2023). CIMIS station data were obtained from their official website: https://cimis.water.ca.gov/WSNReportCriteria.aspx. CARB meteorological data were downloaded from the Air Quality and Meteorological Information System: https://www.arb.ca.gov/aqmis2/metselect.php. LandIQ crop maps were downloaded from the California Department of Water Resources website: https://data.cnra.ca.gov/dataset/statewide-crop-mapping. WRF model source code is available at the official WRF Github repository (NCAR, 2025): https://github.com/wrf-model/WRF. Liljegren's Python-based WBGT code can be freely obtained from the link provided in a published article (Kong & Huber, 2022). Sample Python scripts used to perform data analysis, and produce figures, are made available at the Github repository: https://github.com/psagar123/RuralHeatIsland/ and on Zenodo (Parajuli, 2025).

Acknowledgments

This research is funded by the University of California Office of the President (UCOP) Climate Action Grant award R02CP7521 "Rural heat islands: Mapping and mitigating farmworker exposure to heat stress," PI T. Biggs. SP was funded in part by the SDSU Grants for Established RSCA program. Computational work was carried out on the Expanse supercomputer at the San Diego Supercomputer Center through the NSF ACCESS program.

References

ACGIH. (2017). TLV/BEI Guidelines. In *American Conference of Governmental Hygienists (ACGIH) threshold limit values for chemical substances and physical agents & biological exposure indices*. Retrieved from https://www.acgih.org/science/tlv-bei-guidelines/

Axelson, O. (1974). Influence of heat exposure on productivity. *Work, Environment, Health*, *11*(2), 94–99.

Bernard, T. E., & Barrow, C. A. (2013). Empirical approach to outdoor WBGT from meteorological data and performance of two different instrument designs. *Industrial Health*, *51*(1), 79–85. https://doi.org/10.2486/indhealth.2012-0160

Bonan, G. B. (2008). Forests and climate change: Forcings, feedbacks, and the climate benefits of forests. *Science*, *320*(5882), 1444–1449. https://doi.org/10.1126/science.1155121

Brimicombe, C., Di Napoli, C., Quintino, T., Pappenberger, F., Cornforth, R., & Cloke, H. L. (2022). Thermofeel: A python thermal comfort indices library. *SoftwareX*, *18*, 101005. https://doi.org/10.1016/j.softx.2022.101005

Bröde, P., Fiala, D., Lemke, B., & Kjellstrom, T. (2018). Estimated work ability in warm outdoor environments depends on the chosen heat stress assessment metric. *International Journal of Biometeorology*, *62*(3), 331–345. https://doi.org/10.1007/s00484-017-1346-9

Budd, G. M. (2008). Wet-bulb globe temperature (WBGT)—Its history and its limitations. *Journal of Science and Medicine in Sport*, *11*(1), 20–32. https://doi.org/10.1016/j.jsams.2007.07.003

CCR. (2005). Heat illness prevention in outdoor places of employment (p. 8). Retrieved from https://www.dir.ca.gov/Title8/3395.html

CDFA. (2023). California agricultural production statistics. Retrieved from https://www.cdfa.ca.gov/statistics/

CDWR. (2020). Statewide crop mapping, California Natural Resources Agency Open Data [Dataset]. *California Department of Water Resources*. Retrieved from https://data.cnra.ca.gov/dataset/statewide-crop-mapping

CES. (2020). Current Employment Statistics (CES). Retrieved from https://data.ca.gov/dataset/current-employment-statistics-ces-2

Chakraborty, T., Venter, Z. S., Qian, Y., & Lee, X. (2022). Lower urban humidity moderates outdoor heat stress. *AGU Advances*, *3*(5), e2022AV000729. https://doi.org/10.1029/2022AV000729

Clark, J., & Konrad, C. E. (2024). Observations and estimates of wet-bulb globe temperature in varied microclimates. *Journal of Applied Meteorology and Climatology*, *63*(2), 305–319. https://doi.org/10.1175/JAMC-D-23-0078.1

Cobb, A., Steinhoff, D., Weihs, R., Delle Monache, L., DeHaan, L., Reynolds, D., et al. (2023). West-WRF 34-Year reforecast: Description and validation. *Journal of Hydrometeorology*, *24*(11), 2125–2140. https://doi.org/10.1175/jhm-d-22-0235.1

Collins, D., Della-Marta, P., Plummer, N., & Trewin, B. (2000). Trends in annual frequencies of extreme temperature events in Australia. *Australian Meteorological Magazine*, *49*(4), 277–292. https://doi.org/10.1071/es00025

d'Ambrosio Alfano, F. R., Malchaire, J., Palella, B. I., & Riccio, G. (2014). WBGT index revisited after 60 years of use. *Annals of Occupational Hygiene*, *58*(8), 955–970. https://doi.org/10.1093/annhyg/meu050

Davies, C. T., Brotherhood, J. R., Collins, K. J., Doré, C., Imms, F., Musgrove, J., et al. (1976). Energy expenditure and physiological performance of Sudanese cane cutters. *British Journal of Industrial Medicine*, *33*(3), 181–186. https://doi.org/10.1136/oem.33.3.181

DOA. (2003). *Heat stress control and heat casualty management*. TBMED507/AFPAM (pp. 48–152). Department of the Army and Air Force Technical Bulletin. Retrieved from https://armypubs.army.mil/epubs/DR_pubs/DR_a/ARN35159-TB_MED_507-000-WEB-1.pdf

Dunne, J. P., Stouffer, R. J., & John, J. G. (2013). Reductions in labour capacity from heat stress under climate warming. *Nature Climate Change*, *3*(6), 563–566. https://doi.org/10.1038/nclimate1827

Edholm, O. G., Humphrey, S., Lourie, J. A., Tredre, B. E., Brotherhood, J., & Mourant, A. E. (1973). VI. Energy expenditure and climatic exposure of Yemenite and Kurdish Jews in Israel. *Philosophical Transactions of the Royal Society of London B Biological Sciences*, *266*(876), 127–140. https://doi.org/10.1098/rstb.1973.0042

Fatima, S. H., Rothmore, P., Giles, L. C., Varghese, B. M., & Bi, P. (2021). Extreme heat and occupational injuries in different climate zones: A systematic review and meta-analysis of epidemiological evidence. *Environment International*, *148*, 106384. https://doi.org/10.1016/j.envint.2021.106384

Faucett, J., Meyers, J., Miles, J., Janowitz, I., & Fathallah, F. (2007). Rest break interventions in stoop labor tasks. *Applied Ergonomics*, *38*(2), 219–226. https://doi.org/10.1016/j.apergo.2006.02.003

Graff Zivin, J., & Neidell, M. (2012). The impact of pollution on worker productivity. *The American Economic Review*, *102*(7), 3652–3673. https://doi.org/10.1257/aer.102.7.3652

Grell, G. A., & Freitas, S. R. (2014). A scale and aerosol aware stochastic convective parameterization for weather and air quality modeling. *Atmospheric Chemistry and Physics*, *14*(10), 5233–5250. https://doi.org/10.5194/acp-14-5233-2014

He, C., Valayamkunnath, P., Barlage, M., Chen, F., Gochis, D., Cabell, R., et al. (2023). The community Noah-MP land surface modeling system technical description version 5.0.

Heinzerling, A., Laws, R. L., Frederick, M., Jackson, R., Windham, G., Materna, B., & Harrison, R. (2020). Risk factors for occupational heat-related illness among California workers, 2000–2017. *American Journal of Industrial Medicine*, *63*(12), 1145–1154. https://doi.org/10.1002/ajim.23191

Hersbach, H., Bell, B., Berrisford, P., Biavati, G., Horányi, A., Muñoz Sabater, J., et al. (2023). ERA5 hourly data on pressure levels from 1940 to present. *Copernicus Climate Change Service (C3S) Climate Data Store (CDS)*. https://doi.org/10.24381/cds.bd0915c6

Hersbach, H., Bell, B., Berrisford, P., Hirahara, S., Horányi, A., Muñoz-Sabater, J., et al. (2020). The ERA5 global reanalysis. *Quarterly Journal of the Royal Meteorological Society*, *146*(730), 1999–2049. https://doi.org/10.1002/qj.3803

Hong, S.-Y., Noh, Y., & Dudhia, J. (2006). A new vertical diffusion package with an explicit treatment of entrainment processes. *Monthly Weather Review*, *134*(9), 2318–2341. https://doi.org/10.1175/mwr3199.1

Iacono, M. J., Delamere, J. S., Mlawer, E. J., Shephard, M. W., Clough, S. A., & Collins, W. D. (2008). Radiative forcing by long-lived greenhouse gases: Calculations with the AER radiative transfer models. *Journal of Geophysical Research*, *113*(D13), D13103. https://doi.org/10.1029/2008jd009944

ICFB. (2024). Imperial Valley Harvest Calendar. Retrieved from https://ucanr.edu/sites/drecBETA/files/370274.pdf

ISO. (2017). *7243: Ergonomics of the thermal environment—Assessment of heat stress using the WBGT (wet bulb globe temperature) index*. International Organization for Standardization.

Jacklitsch, B. L., Williams, W. J., Musolin, K., Coca, A., Kim, J.-H., & Turner, N. (2016). Occupational exposure to heat and hot environments: Revised criteria 2016. https://www.cdc.gov/niosh/docs/2016-106/default.html

Jackson, L. L., & Rosenberg, H. R. (2010). Preventing heat-related illness among agricultural workers. *Journal of Agromedicine*, *15*(3), 200–215. https://doi.org/10.1080/1059924x.2010.487021

Jiménez, P. A., Dudhia, J., González-Rouco, J. F., Navarro, J., Montávez, J. P., & García-Bustamante, E. (2012). A revised scheme for the WRF surface layer formulation. *Monthly Weather Review*, *140*(3), 898–918. https://doi.org/10.1175/mwr-d-11-00056.1

Kamai, E. M., Ruiz, B. C., Van Horne, Y. O., Barahona, D. D., Bejarano, E., Olmedo, L., et al. (2023). Agricultural burning in Imperial Valley, California and respiratory symptoms in children: A cross-sectional, repeated measures analysis. *Science of the Total Environment*, *901*, 165854. https://doi.org/10.1016/j.scitotenv.2023.165854

Kjellstrom, T., Freyberg, C., Lemke, B., Otto, M., & Briggs, D. (2018). Estimating population heat exposure and impacts on working people in conjunction with climate change. *International Journal of Biometeorology*, *62*(3), 291–306. https://doi.org/10.1007/s00484-017-1407-0

Kjellstrom, T., Holmer, I., & Lemke, B. (2009). Workplace heat stress, health and productivity – An increasing challenge for low and middle-income countries during climate change. *Global Health Action*, *2*(1), 2047. https://doi.org/10.3402/gha.v2i0.2047

Kjellstrom, T., Lemke, B., Otto, M., Hyatt, O., & Dear, K. (2014). *Occupational heat stress: Contribution to WHO project on "Global assessment of the health impacts of climate change", which started in 2009* (Vol. 4). Health and Environment International Trust.

Kong, Q., & Huber, M. (2022). Explicit calculations of wet-bulb globe temperature compared with approximations and why it matters for labor productivity. *Earth's Future*, *10*(3), e2021EF002334. https://doi.org/10.1029/2021EF002334

Kong, Q., & Huber, M. (2024). A new, zero-iteration analytic implementation of wet-bulb globe temperature: Development, validation, and comparison with other methods. *GeoHealth*, *8*(10), e2024GH001068. https://doi.org/10.1029/2024GH001068

Liljegren, J. C., Carhart, R. A., Lawday, P., Tschopp, S., & Sharp, R. (2008). Modeling the wet bulb globe temperature using standard meteorological measurements. *Journal of Occupational and Environmental Hygiene*, *5*(10), 645–655. https://doi.org/10.1080/15459620802310770

Malchaire, J. B. (1979). The TLV work—Rest regimens for occupational exposure to heat: A review of their development. *Annals of Occupational Hygiene*, *22*(1), 55–62. https://doi.org/10.1093/annhyg/22.1.55

Martin, P. L., Hooker, B., Akhtar, M., & Stockton, M. (2017). How many workers are employed in California agriculture? *California Agriculture*, *71*(1).

Matsumoto, K. I., Tachiiri, K., & Su, X. (2021). Heat stress, labor productivity, and economic impacts: Analysis of climate change impacts using two-way coupled modeling. *Environmental Research Communications*, *3*(12), 125001. https://doi.org/10.1088/2515-7620/ac3e14

Mayer, A. (2023). Nighttime harvests can protect farmworkers from blistering heat, but they bring new risks. Retrieved from https://www.eater.com/2023/10/12/23906597/labor-farm-nighttime-harvests-protect-workers-heat-risk

Mitchell, D. C., Castro, J., Armitage, T. L., Tancredi, D. J., Bennett, D. H., & Schenker, M. B. (2018). Physical activity and common tasks of California farm workers: California Heat Illness Prevention Study (CHIPS). *Journal of Occupational and Environmental Hygiene*, *15*(12), 857–869. https://doi.org/10.1080/15459624.2018.1519319

Mohammadian, M., Heidari, H., Charkhloo, E., & Dehghani, A. (2020). Heat stress and physiological and perceptual strains of date harvesting workers in palm groves in Jiroft. *Work*, *66*(3), 625–636. https://doi.org/10.3233/wor-203205

Morris, C. E., Gonzales, R. G., Hodgson, M. J., & Tustin, A. W. (2019). Actual and simulated weather data to evaluate wet bulb globe temperature and heat index as alerts for occupational heat-related illness. *Journal of Occupational and Environmental Hygiene*, *16*(1), 54–65. https://doi.org/10.1080/15459624.2018.1532574

Morrison, H., Thompson, G., & Tatarskii, V. (2009). Impact of cloud microphysics on the development of trailing stratiform precipitation in a simulated squall line: Comparison of one-and two-moment schemes. *Monthly Weather Review*, *137*(3), 991–1007. https://doi.org/10.1175/2008mwr2556.1

Moyce, S., Mitchell, D., Armitage, T., Tancredi, D., Joseph, J., & Schenker, M. (2017). Heat strain, volume depletion and kidney function in California agricultural workers. *Occupational and Environmental Medicine*, *74*(6), 402–409. https://doi.org/10.1136/oemed-2016-103848

NCAR. (2025). WRF-ARW modeling System [Software]. *GitHub*. Retrieved from https://github.com/wrf-model/WRF

NWS. (2023). *Wet bulb globe temperature suggested actions and impact prevention*. National Weather Service. Retrieved from https://www.weather.gov/ict/wbgt

Ostro, B. D., Roth, L. A., Green, R. S., & Basu, R. (2009). Estimating the mortality effect of the July 2006 California heat wave. *Environmental Research*, *109*(5), 614–619. https://doi.org/10.1016/j.envres.2009.03.010

Pan, Q., Sumner, D. A., Mitchell, D. C., & Schenker, M. (2021). Compensation incentives and heat exposure affect farm worker effort. *PLoS One*, *16*(11), e0259459. https://doi.org/10.1371/journal.pone.0259459

Parajuli, S. (2025). Rural heat Island [Software]. *Zenodo*. https://doi.org/10.5281/zenodo.18276094

Parajuli, S. P., Biggs, T., de Sales, F., Zavala Perez, M. A., He, C., Jones, C., et al. (2024). Impact of irrigation on farmworkers' heat stress in California differs by season and during the day and night. *Communications Earth & Environment*, *5*(1), 787. https://doi.org/10.1038/s43247-024-01959-7

Parajuli, S. P., Biggs, T., Galvez, N. L., Quintana, P., Ciborowski, H., De Sales, F., et al. (2025). Heat-related rest-break recommendations for farmworkers in California based on wet-bulb globe temperature. *Communications Earth & Environment*, *6*(1), 359. https://doi.org/10.1038/s43247-025-02327-9

Parajuli, S. P., Stenchikov, G. L., Ukhov, A., Mostamandi, S., Kucera, P. A., Axisa, D., et al. (2022). Effect of dust on rainfall over the Red Sea coast based on WRF-Chem model simulations. *Atmospheric Chemistry and Physics*, *22*(13), 8659–8682. https://doi.org/10.5194/acp-22-8659-2022

Parajuli, S. P., & Yang, Z.-L. (2017). Understanding dust emission in the Bodélé region by extracting locally mobilized dust aerosols from satellite Aerosol Optical Depth data using principal component analysis. *Aeolian Research*, *24*, 105–113. https://doi.org/10.1016/j.aeolia.2017.01.001

Parsons, L. A., Masuda, Y. J., Kroeger, T., Shindell, D., Wolff, N. H., & Spector, J. T. (2022). Global labor loss due to humid heat exposure underestimated for outdoor workers. *Environmental Research Letters*, *17*(1), 014050. https://doi.org/10.1088/1748-9326/ac3dae

Poulianiti, K. P., Havenith, G., & Flouris, A. D. (2019). Metabolic energy cost of workers in agriculture, construction, manufacturing, tourism, and transportation industries. *Industrial Health*, *57*(3), 283–305. https://doi.org/10.2486/indhealth.2018-0075

Rasmussen, R., Chen, F., Liu, C., Ikeda, K., Prein, A., Kim, J., et al. (2023). CONUS404: The NCAR–USGS 4-km long-term regional hydroclimate reanalysis over the CONUS. *Bulletin of the American Meteorological Society*, *104*(8), E1382–E1408. https://doi.org/10.1175/bams-d-21-0326.1

Roson, R., & Sartori, M. (2016). Estimation of climate change damage functions for 140 regions in the GTAP9 database. *SSRN Electronic Journal*. https://doi.org/10.2139/ssrn.2741588

Rothfusz, L. P. (1990). The heat index equation (or, more than you ever wanted to know about heat index). https://unidata.github.io/MetPy/latest/_static/rothfusz-1990-heat-index-equation.pdf

Saeed, W., Haqiqi, I., Kong, Q., Huber, M., Buzan, J. R., Chonabayashi, S., et al. (2022). The poverty impacts of labor heat stress in West Africa under a warming climate. *Earth's Future*, *10*(11), e2022EF002777. https://doi.org/10.1029/2022EF002777

Sahu, S., Sett, M., & Kjellstrom, T. (2013). Heat exposure, cardiovascular stress and work productivity in rice harvesters in India: Implications for a climate change future. *Industrial Health*, *51*(4), 424–431. https://doi.org/10.2486/indhealth.2013-0006

Smith, D. J., Pius, L. M., Plantinga, L. C., Thompson, L. M., Mac, V., & Hertzberg, V. S. (2022). Heat stress and kidney function in farmworkers in the US: A scoping review. *Journal of Agromedicine*, *27*(2), 183–192. https://doi.org/10.1080/1059924x.2021.1893883

Tan, E., & Bogage, J. (2023). Extreme heat is forcing America's farmers to go nocturnal. *The Washington Post*. https://link.gale.com/apps/doc/A764445815/AONE?u=san96005&sid=googleScholar&xid=6171bfa8

Tawatsupa, B., Yiengprugsawan, V., Kjellstrom, T., Berecki-Gisolf, J., Seubsman, S.-A., & Sleigh, A. (2013). Association between heat stress and occupational injury among Thai workers: Findings of the Thai cohort Study. *Industrial Health*, *51*(1), 34–46. https://doi.org/10.2486/indhealth.2012-0138

Thompson, C. F., Jones, C., Biggs, T., Quintana, P. J. E., Perez, M. A. Z., De Sales, F., et al. (2025). A climatology of summertime wet-bulb globe temperature in California's imperial Valley. *Journal of Applied Meteorology and Climatology*, *64*(7), 911–932. https://doi.org/10.1175/JAMC-D-24-0199.1

Valayamkunnath, P. (2019). *Understanding the role of vegetation dynamics and anthropogenic induced changes on the terrestrial water cycle*. Virginia Tech.

Vargo, J., Xiao, Q., & Liu, Y. (2015). The performance of the national weather service heat warning system against ground observations and satellite imagery. *Advances in Meteorology*, *2015*(1), 649614–649615. https://doi.org/10.1155/2015/649614

Vecellio, D. J., Kong, Q., Kenney, W. L., & Huber, M. (2023). Greatly enhanced risk to humans as a consequence of empirically determined lower moist heat stress tolerance. *Proceedings of the National Academy of Sciences*, *120*(42), e2305427120. https://doi.org/10.1073/pnas.2305427120

Vega-Arroyo, A. J., Mitchell, D. C., Castro, J. R., Armitage, T. L., Tancredi, D. J., Bennett, D. H., & Schenker, M. B. (2019). Impacts of weather, work rate, hydration, and clothing in heat-related illness in California farmworkers. *American Journal of Industrial Medicine*, *62*(12), 1038–1046. https://doi.org/10.1002/ajim.22973

Ward, A., Clark, J., McLeod, J., Woodul, R., Moser, H., & Konrad, C. (2019). The impact of heat exposure on reduced gestational age in pregnant women in North Carolina, 2011–2015. *International Journal of Biometeorology*, *63*(12), 1611–1620. https://doi.org/10.1007/s00484-019-01773-3

WMO. (2016). *Guidelines on the definition and monitoring of extreme weather and climate events*. TT-DEWCE WMO.

Wyndham, C. H. (1969). Adaptation to heat and cold. *Environmental Research*, *2*(5), 442–469. https://doi.org/10.1016/0013-9351(69)90015-2

Yaglou, C., & Minard, D. (1957). Control of heat casualties at military training centers. *Archives of Industrial Health*, *16*(4), 302–316.

Zhao, L., Oleson, K., Bou-Zeid, E., Krayenhoff, E. S., Bray, A., Zhu, Q., et al. (2021). Global multi-model projections of local urban climates. *Nature Climate Change*, *11*(2), 152–157. https://doi.org/10.1038/s41558-020-00958-8